

EHD gas flow in electrostatic levitation unit

L. Zhao, K. Adamiak*

Department of Electrical and Computer Engineering, The University of Western Ontario, London, Ontario, Canada N6A 5B9

Available online 8 November 2005

Abstract

This paper presents the results of numerical simulation for an electrostatic levitation device. An algorithm, based on the Boundary and Finite Element Methods, and the Method of Characteristics, was employed to predict the electric field. The FLUENT software was used to calculate the airflow. Detailed distributions of different parameters have been presented. The results seem to confirm the feasibility of the concept of electrostatic levitating unit.

© 2005 Elsevier B.V. All rights reserved.

Keywords: Corona discharge; Electrohydrodynamics; Airflow; Electrostatic levitation device; Electric field

1. Introduction

The electrostatic levitation device, or lifter, was first suggested by Brown [1]. Its potential advantages are that it works without moving parts, is silent, and—theoretically—is able to lift not only its own weight but also an additional load. Until now, more than 250 lifter replications have been successfully fabricated by many researchers and (mostly) hobbyists worldwide [2]. However, despite numerous experimental attempts, not much effort has been made to gain a better theoretical understanding of the levitation mechanism.

Rare publications on this subject have resorted to less known physical phenomena [3,4]. For example Musha [3] tried to use the Biefeld-Brown effect to explain the generation of the lifting force. Apparently, the authors working in this area did not correlate this device with—once well-known, but now partially forgotten—designs of the corona electrostatic motors [5]. The goal of this paper is to explain the mechanism of generating the levitation force by investigating the corona discharge and the secondary electrohydrodynamic (EHD) flow in a system of two parallel electrodes.

2. Design of electrostatic levitation unit

The electrostatic levitation device studied in this paper consists of two mechanically connected electrodes: a thin corona wire that is parallel to a much thicker ground electrode without any sharp points (Fig. 1). These two electrodes form a triangular (although many other shapes are also possible) structure with spacers made of light wood or hollow plastic tubes. These spacers should also be out of good insulating materials, so that high voltage applied between both electrodes does not produce any measurable leaking current.

When a high voltage is applied between these two electrodes the electric corona discharge is generated. The high electric field in the vicinity of the corona electrode causes gas ionization and its partial breakdown; as a result ions drift to the ground electrode. A space charge is formed and an electric current flows between both electrodes [6].

Generation of the levitation force is explained in the theoretical model of the problem, shown in Fig. 2. Just one pair of the electrodes is taken into account assuming that they are infinitely long. All other elements are neglected, as they do not contribute to the force generation. By considering the symmetry of the system and neglecting the edge effect, a 2D model can be assumed. Examples of the system parameters are also shown.

Fig. 3a shows all electric forces involved. The corona wire, supplied with a positive voltage, experiences a repulsive force F_{1i} due to the positive space charge and

*Corresponding author. Tel.: +519 661 2111x88358; fax: +519 850 2436.

E-mail address: kadamiak@eng.uwo.ca (K. Adamiak).

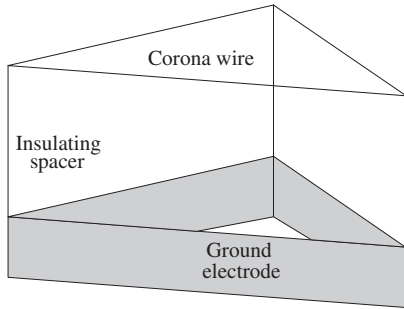


Fig. 1. The configuration of the electrostatic lifter.

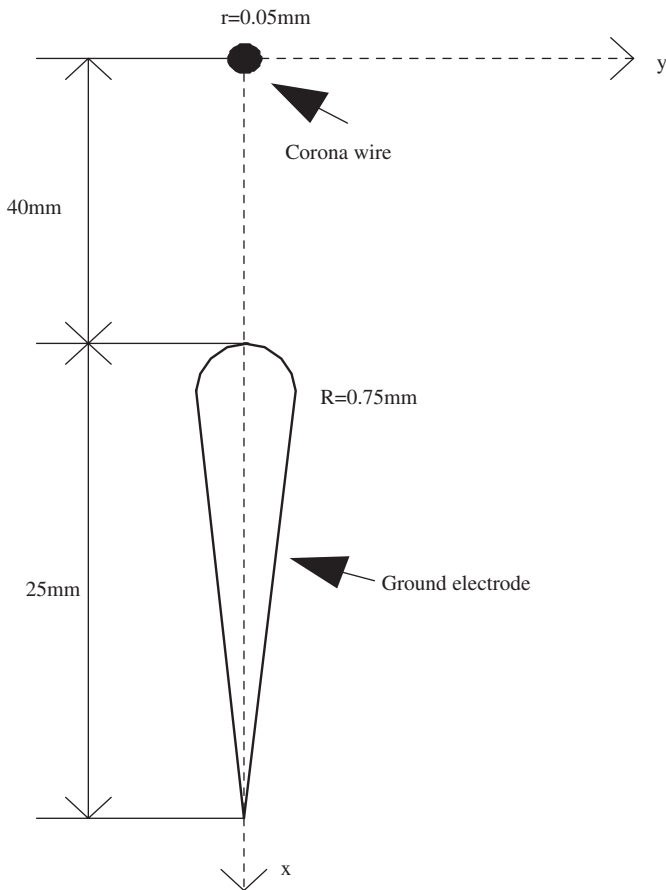


Fig. 2. The simplified model of the electrostatic lifter.

an attractive force $-F_e$ due to the ground electrode. Similarly, a force $F_{1i} + F_{2i}$ acts on the positive space charge due to attraction to both electrodes, while $F_{2i} + F_e$ acts on the ground electrode because of the space charge and the corona electrode. Treating electrodes and the space charge as one system, the net force is zero. However, the movement of ions in the corona discharge is obstructed by the collisions with electrically neutral air molecules; the frequency of the collisions being so high that the complete momentum transfer from the ionic space charge to the air bulk can be assumed to take place. Therefore, the Coulomb force acting on the ions becomes an electric body force on the air molecules and gives rise to the EHD flow [6].

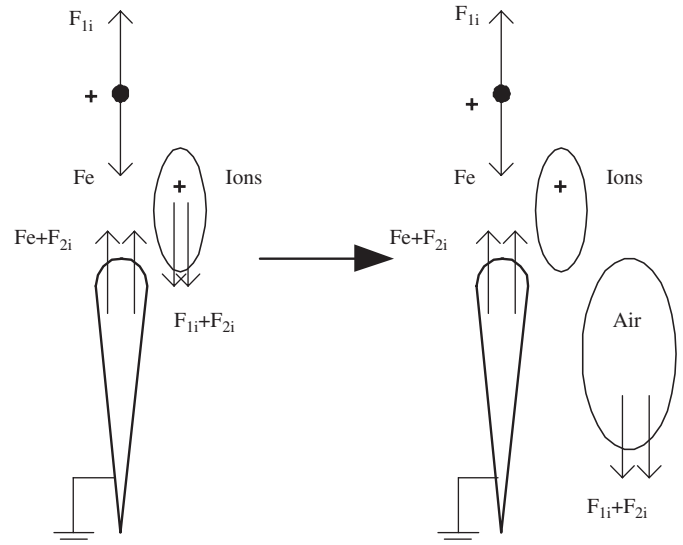


Fig. 3. Electric forces in the lifter without (a) and with (b) air.

Fig. 3b shows this stage with the ions having given up their force to the air molecules; now the net force on the system is $F_{1i} + F_{2i}$, which is the reaction force to the one that drives the airflow. Therefore, this force causes the system levitation. There are also other forces acting on both electrodes, most importantly the viscous drag and pressure forces. The levitation effect can be achieved if the sum of all of the forces is larger than the gravitational force.

3. Numerical model

3.1. Electric model

A simplified model of the corona discharge has been assumed in this study, where the thickness of the ionization layer is so small that it can be neglected—only one species of the electric ions is injected from the ionization layer to the air gap between the two electrodes and form a space charge. It is also assumed that the corona discharge is unipolar and stationary. In this case the electric field is governed by the well-known Poisson equation:

$$\nabla^2 \Phi = -\frac{q}{\epsilon}, \tag{1}$$

where Φ is the scalar electric potential, q the space charge density and ϵ the permittivity of the ambient gas.

The ionic charges are accelerated by the Coulomb force and move towards the ground plate. The charge drift creates an electric current with a density defined as

$$\vec{j} = q(K\vec{E} + \vec{v}) - D\nabla q, \tag{2}$$

where \vec{j} is the current density, K the mobility of ions, D the ions diffusion coefficient and \vec{v} the gas velocity. Under steady state conditions, the current density must satisfy the

charge conservation equation.

$$\nabla \cdot \vec{j} = 0. \quad (3)$$

Since the drift velocity of ions is usually approximately two orders of magnitude bigger than the typical velocity of the gas flow [7], the convective component in the ionic current density can be neglected, therefore $\vec{j} = Kq\vec{E} - D\nabla q$. Under such an assumption, and after neglecting the ion diffusion, the charge conservation Eq. (3) leads to [8]:

$$\nabla q \cdot \nabla \Phi = q^2/\epsilon. \quad (4)$$

Therefore, the electric problem of the corona discharge is governed by a set of two partial differential equations with two unknown distributions: the linear one (1) with the unknown potential Φ and the non-linear one (4) with the unknown space charge density q . The boundary conditions should also be specified and for the potential are very straightforward: a given DC potential Φ_0 at the corona electrode and zero at the ground one.

However, the formulation of proper boundary conditions for the space charge density is not as easy, which is a simple consequence of neglecting the ionization layer. The Kaptzov hypothesis—which suggests that the electric field increases proportionally to the voltage below the corona onset level, but will preserve its value after the corona is initiated—is usually adopted. Peek's formula is used to determine the threshold strength of electric field for the corona onset at the corona electrode [9]. This approach provides an indirect boundary condition for space charge density; its distribution on the corona electrode surface is iterated until the corona electrode electric field is sufficiently close to Peek's value [10].

Adopting direct ionization criteria provides another option [11]. This technique is much more time consuming and complicated, but the final effect is very similar to the one described above.

3.2. Air flow model

Under the assumption that the ambient air is incompressible, has constant density and viscosity, and the flow is steady and laminar, the airflow has to satisfy the continuity equation:

$$\nabla \cdot \vec{v} = 0 \quad (5)$$

and the Navier–Stokes equation:

$$\nabla \cdot (\rho \vec{v} \vec{v}) = -\nabla P + \nabla \cdot (\bar{\tau}) + \vec{F}, \quad (6)$$

where ρ is the gas density, P the static pressure, \vec{F} the external body force, in this case equal to the Coulomb force $q\nabla\Phi$, and $\bar{\tau}$ the stress tensor.

$$\bar{\tau} = \eta \left[(\nabla \vec{v} + \nabla \vec{v}^T) - \frac{2}{3} \nabla \cdot \vec{v} I \right], \quad (7)$$

where η is the air viscosity and I the unit tensor.

The boundary conditions for the airflow are straightforward: the two electrodes act as stationary walls where both

axial and radial components of the velocity vector vanish; the outside boundary of the domain is defined as pressure-inlet and pressure-outlet with the relative pressure equal to zero and the direction of the back flow normal to the boundary, since the computational domain is open in this area and air is free to flow in both directions.

4. Numerical simulation

The numerical algorithm involves two separate problems: an ionized electric field and gas flow. The first one has been solved in our own computer software, while the commercial FLUENT software was used for the gas flow problem. Domain discretization was identical in both and was obtained by the commercial software GAMBIT. Typically, about 24000 triangular cells and 12000 nodes have been generated with a very non-uniform density: the elements close to the thin corona wire were much smaller than in other places, especially far from both electrodes.

The user-defined functions (UDF) were used to provide a link between both computer programs—electrical body force was entered into every single volume cell of the discretized FLUENT model [12].

4.1. Electric field

The numerical algorithm for the corona discharge simulation is based on three different numerical techniques: BEM, FEM and MOC. The BEM is used to obtain the solution of the Laplacian electric field where space charge is assumed to be zero and only the applied voltage between the two electrodes is considered. The electric field gradient is very high in the vicinity of the corona electrode and the BEM can provide very accurate and smooth solution in this area without creating an algebraic system that is too large. In the next step, the conventional FEM procedure is employed to obtain the Poissonian component of the electric potential where the space charge is considered and both electrodes are at ground potential. The final solution for Φ is the superposition of the BEM and the FEM components. The electric field can be easily calculated by differentiating the potential distribution. The last step is to solve the space charge density by MOC [8,9].

The algorithm is arranged in a double iterative loop. The inner loop starts from some initial guess of the space charge density, and Eqs. (1) and (4) are solved iteratively for Φ and q . The outer loop is added to update the charge density on the corona electrode surface until the electric field values there are sufficiently close to Peek's value [10]. All local parameters of the electric corona discharge process, including the space charge density, the current density, the electric field and the potential for every point in the simulation domain can be obtained.

Figs. 4 and 5 display the potential and the space charge density distributions in the air gap between both electrodes. With the corona wire at 35 kV and the other electrode at the ground potential, the potential changes smoothly at the

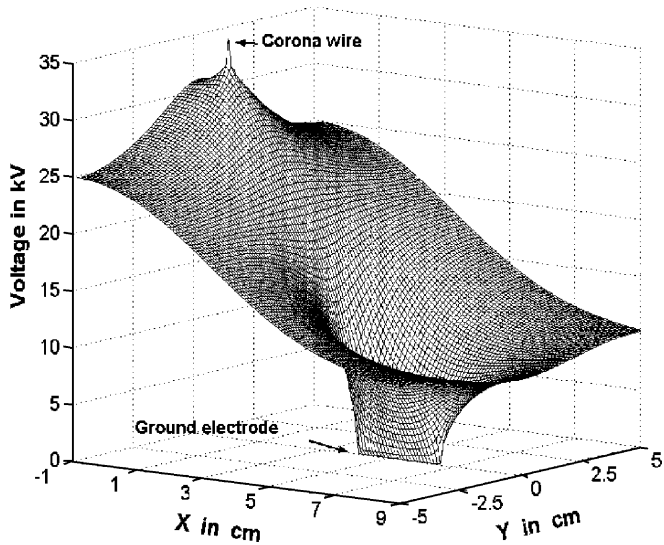


Fig. 4. Potential distribution at 35 kV.

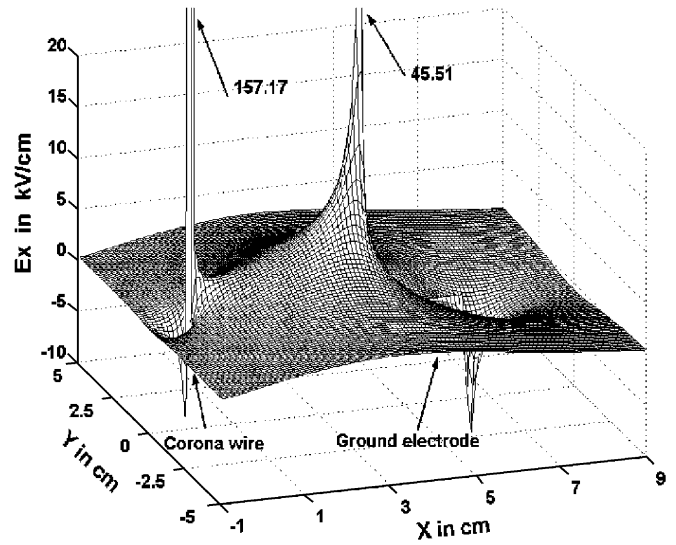


Fig. 6. Longitudinal component of the electric field at 35 kV.

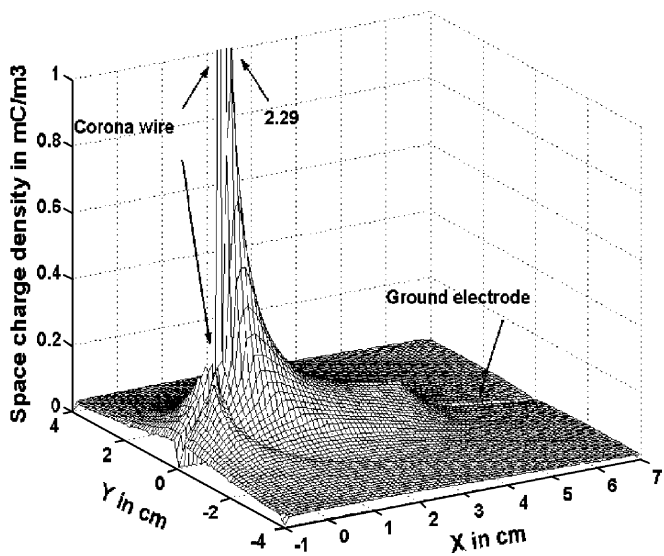


Fig. 5. Space charge density distribution at 35 kV.

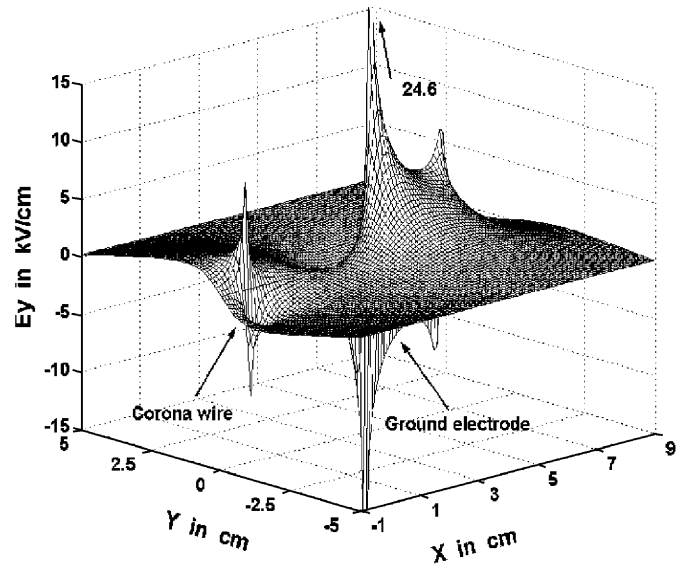


Fig. 7. Transverse component of the electric field at 35 kV.

majority of points in the air gap except for the dramatic changes near the corona wire and the ground electrode. The maximum value of space charge density is 2.29 mC/m^3 at the point located at the intersection of the wire surface and the axis of the symmetry ($y=0$). Then the space charge density decreases quickly towards the ground electrode. Almost all of the space charge accumulates at a narrow channel linking both electrodes and centered along the axis of the symmetry. Still, some space charge density is present at all points on the surface of the corona wire, what means that at 35 kV the corona discharge takes place at all wire points, even on the other side of the ground electrode. However, the space charge density decreases very quickly in the negative x direction.

The electric field is very strong on the surface of the corona wire and the other electrode, especially at the points facing the opposite electrode (Figs. 6 and 7). The most intensive gas ionization can be expected at these points. The presence of the space charge tends to decrease the electric field near the corona wire and increase it near the ground electrode.

The Coulomb force, driving the air motion, is a product of the electric field and the space charge density. Both components of this force are shown in Figs. 8 and 9. The gradient of the voltage near the wire is much higher than in other places, so the electric field reaches very high values at these points; therefore the Coulomb force is also very strong. The longitudinal component of the force dominates over the transverse one with the strongest values located in

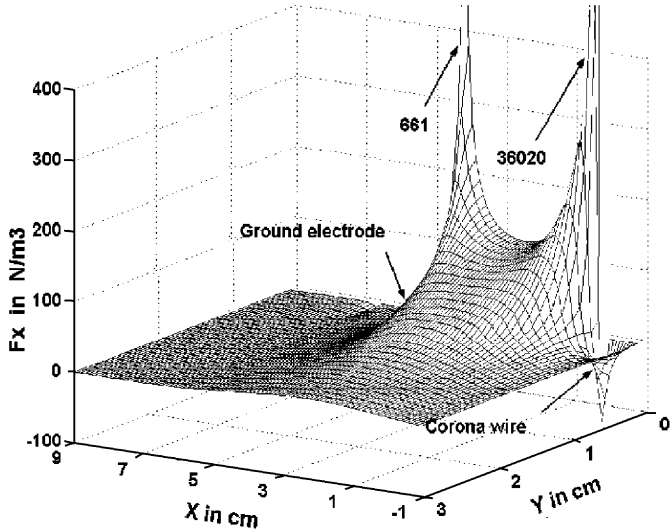


Fig. 8. Longitudinal component of the Coulomb force density at 35 kV.

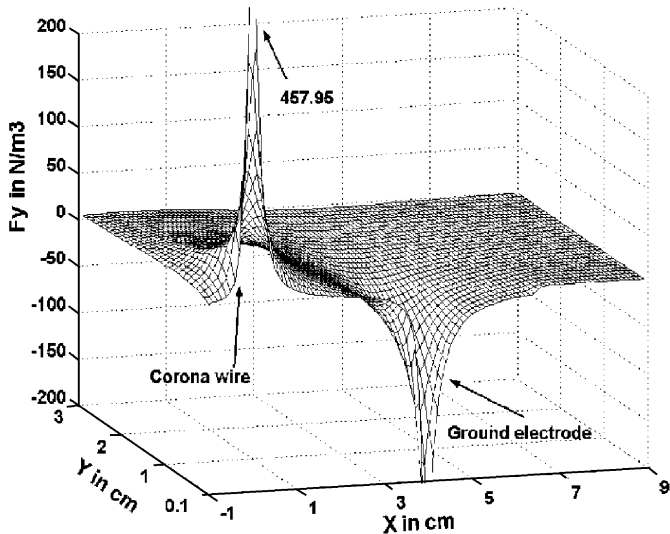


Fig. 9. Transverse component of the Coulomb force density at 35 kV.

a narrow band between the two electrodes, what means that F_x will play the key role in driving the airflow. In this situation the airflow will be mostly parallel to the x -axis and will provide a thrust force similar to that of a rocket.

Although the longitudinal component of the electric field E_x has negative values both in the area above the corona wire and below the ground electrode, where the electric field lines point in the negative x direction, the electric force F_x has noticeable negative value only above the corona electrode because of negligible space charge density below the ground electrode. The presence of the negative force reduces the flow velocity, but these negative values are extremely small as compared to the positive ones and they are located in a very limited area above the corona wire.

Both transversal electric field E_y , and transversal force F_y , are zero on the x -axis ($y = 0$), because of the symmetry of

the system. However, these values have been excluded from Fig. 9 in order to improve visibility of the graph.

4.2. Air flow

The FLUENT commercial software was used to perform the numerical simulation of the airflow. The governing partial differential Eqs. (5)–(7) are solved using the Finite Volume Method: a control-volume-based technique is used to convert these equations into a set of algebraic equations that can be solved numerically. This control volume technique integrates the governing equations over each control volume, yielding discrete equations that conserve each quantity on a control-volume basis. Typically, a few hundred iterations are needed for the program to converge.

Figs. 10 and 11 present the airflow velocity distributions in x and y directions, respectively. It can be noticed that the scale of the velocity is m/s, which explains the noticeable wind noise during the levitation experiment [2]. In the longitudinal x direction, the air is accelerated by the x component of the Coulomb force from the corona wire towards the ground electrode, so that the longitudinal velocity increases in the x direction. Since the ground electrode acts as a stationary wall, v_x decreases to zero on this surface. Then, the airflow is deflected and forced to follow along the outer surface of the wall.

In the transverse direction, the air is drawn towards the symmetry plane to supplement the air that flows towards the ground electrode, what explains the negative values of this component near the corona wire. Close to the ground electrode the airflow is forced to change its direction, producing large values of the transverse velocity near the ground electrode.

The relative pressure distribution shown in Fig. 12 is consistent with the velocity distribution. It is clear that part of the wire surface that faces the ground electrode experiences the maximum negative relative pressure because of the highest acceleration of gas molecules and the

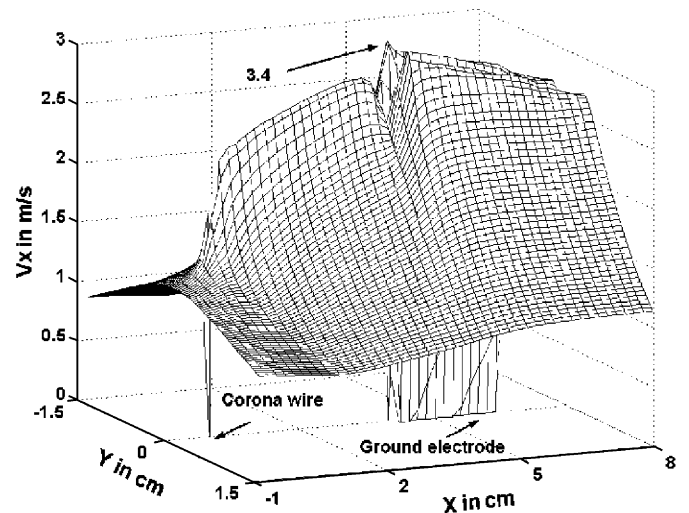


Fig. 10. Longitudinal component of airflow velocity distribution at 35 kV.

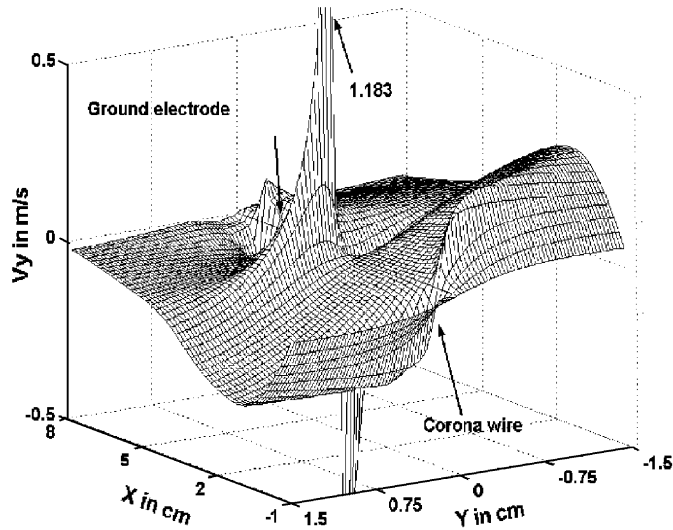


Fig. 11. Transverse component of airflow velocity distribution at 35 kV.

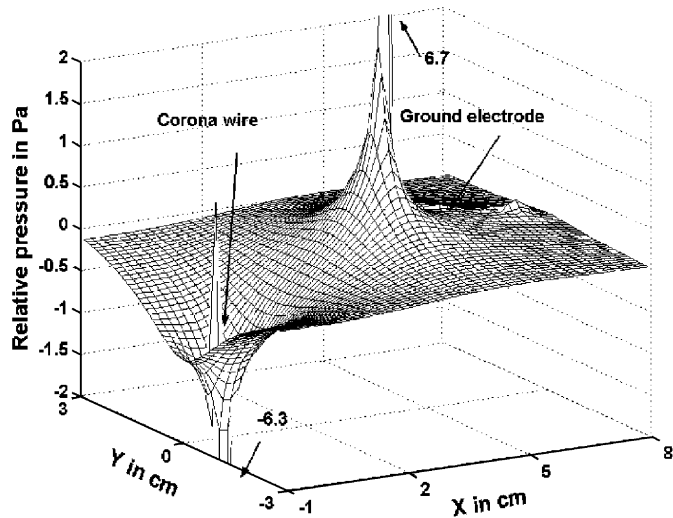


Fig. 12. Relative pressure distribution at 35 kV.

large x -component of the velocity vector. On the other hand, the maximum positive relative pressure occurs at the central point of the ground electrode, where the longitudinal velocity decreases to zero and the airflow is forced to change its direction.

5. Calculation of forces

As mentioned before, the main factors involved in the electrostatic levitation system are the x -components of the Coulomb, viscous drag and pressure-generated forces resulting from the moving air. Although the forces in the y direction are also contributing to the airflow, they cancel each other because of the system symmetry and because only the longitudinal forces contribute to the levitation phenomenon.

Table 1
Longitudinal forces in the levitation unit

	F_{px} (N/m)	F_{vx} (N/m)	Total (N/m)	F_{cx} (N/m)
Corona wire	0.00029	0.00019	0.00048	-0.163
Ground electrode	0.00266	0.00352	0.00618	
Net force	0.00295	0.00371	0.00666	-0.156

In order to calculate the x -component of Coulomb force (F_{cx}), it is necessary to integrate the force density (Fig. 8) over the whole computational domain. The total pressure-generated forces (F_{px}) in the x direction on both electrodes can be calculated by summing the pressure forces on each section of the electrode according to the equation:

$$\vec{F}_P = - \sum_{i=1}^n \hat{x} \cdot (P_i - P_{\text{ref}}) A_i \hat{n}_i, \quad (8)$$

where n is the number of sections on the electrode, A the area of the section, P pressure, P_{ref} reference pressure, \hat{x} the x unit vector and \hat{n} the unit vector normal to the face. A similar equation:

$$\vec{F}_{vx} = \sum_{i=1}^n \hat{x} \cdot \bar{\tau}_i A_i \hat{n}_i \quad (9)$$

can be applied to the calculation of the viscosity related forces (F_{vx}) on the electrodes, where $\bar{\tau}$ is the stress tensor for the section.

The results of calculations are presented in Table 1, which shows all forces in the x direction, per unit length of the device, assuming that the potential difference between both electrodes is 35 kV. The net force is 0.156 N/m in the negative x direction, so if the corona wire is positioned above the ground plate there should be the levitation effect. At this voltage level a weight of 15.9 g, which may include lifter's own weight and an additional payload, can be lifted.

6. Conclusions

The paper presents the results of a numerical simulation of an electrostatic levitation system. Contrary to some other researchers, who resorted to some less known physical principles, the secondary electrohydrodynamic flow has been used to explain the generation of the levitation force.

A numerical algorithm is presented, which can be used to predict the EHD flow in air produced by the electric corona discharge between two electrodes of the electrostatic levitation system. This algorithm comprises two stages: first, the distributions of the electric field, the electric potential and the charge density are calculated using a hybrid technique based on the Boundary and Finite Element Methods, and the Method of Characteristics. Then, the Coulomb force is entered into the airflow simulation by user-defined-functions of the commercial

FLUENT software. The airflow velocity and the relative pressure distributions are predicted.

Based on the simulation results, both of the electric field and the airflow, three different forces, the Coulomb force, the viscous drag and pressure-generated forces, have been calculated. The final net force confirms the feasibility of the levitation idea, assuming that the whole device is not too heavy.

References

- [1] T.T. Brown, Electrokinetic Apparatus, US Patent N°2949550, 1960.
- [2] <http://jnaudin.free.fr/lifters/main.htm>.
- [3] T. Musha, I. Abe, Biefeld-Brown effect and electrogravitational propulsion by high potential electric field, in: Proceedings of the 24th JSASS Annual Meeting, 1993, pp. 189–192.
- [4] T.B. Bahder, C. Fazi, Force on an asymmetrical capacitor, Army Research Laboratory, Report No. ARL-TR-3005, March 2003, pp. 1–31.
- [5] O.D. Jefimienko, Electrostatic motors, in: A.D. Moore (Ed.), *Electrostatics and its Applications*, Wiley, New York, 1973, pp. 131–147.
- [6] J.D. Cobine, *Gaseous Conductors*, Dover, New York, 1958.
- [7] T. Yamamoto, H.R. Velkoff, Electrohydrodynamics in an electrostatic precipitator, *J. Fluid Mech.* 108 (1981) 1–18.
- [8] K. Adamiak, P. Atten, Simulation of corona discharge in point-plane configuration, in: Proceedings of the ESA-IEEE Joint Meeting on Electrostatics, 2003, pp. 104–118.
- [9] K. Adamiak, J. Zhang, L. Zhao, Finite element versus hybrid BEM-FEM techniques for the electric corona simulation, *Electrotech. Rev.* 10 (2003) 753–756.
- [10] A.M. Meroth, T. Gerber, C.D. Munz, P.L. Levin, A.J. Schwab, Numerical solution of nonstationary charge coupled problems, *J. Electrostat.* 45 (1999) 177–198.
- [11] K. Adamiak, P. Atten, V. Atrazhev, Electric corona discharge in the hyperbolic point—ground plate configuration, 2002 Annual Report Conference on Electrical Insulation and Dielectric Phenomena, Cancun, Mexico, 2002, pp. 109–112.
- [12] L. Zhao, K. Adamiak, EHD flow in air produced by electric corona discharge in pin-plate configuration, *J. Electrostat.* 63 (2004) 337–350.